LETTERS
PUBLISHED ONLINE: 15 MARCH 2009 | DOI: 10.1038/NGEO462
nature geoscience

Model projections of rapid sea-level rise on the northeast coast of the United States

Jianjun Yin[1]*, Michael E. Schlesinger[2] and Ronald J. Stouffer[3]

Human-induced climate change could cause global sea-level rise. Through the dynamic adjustment of the sea surface in response to a possible slowdown of the Atlantic meridional overturning circulation[1,2], a warming climate could also affect regional sea levels, especially in the North Atlantic region[3], leading to high vulnerability for low-lying Florida and western Europe[4–6]. Here we analyse climate projections from a set of state-of-the-art climate models for such regional changes, and find a rapid dynamical rise in sea level on the northeast coast of the United States during the twenty-first century. For New York City, the rise due to ocean circulation changes amounts to 15, 20 and 21 cm for scenarios with low, medium and high rates of emissions respectively, at a similar magnitude to expected global thermal expansion. Analysing one of the climate models in detail, we find that a dynamic, regional rise in sea level is induced by a weakening meridional overturning circulation in the Atlantic Ocean, and superimposed on the global mean sea-level rise. We conclude that together, future changes in sea level and ocean circulation will have a greater effect on the heavily populated northeastern United States than estimated previously[7–9].

In the current climate, sea level is anomalously low along the east coast of the United States, with a steep sea-level slope just offshore. This sharp sea surface height (SSH) gradient is required by geostrophy (the balance between Coriolis and pressure-gradient forces) to maintain the strong and narrow Gulf Stream and North Atlantic Current, which are components of the Atlantic meridional overturning circulation (AMOC). The high-latitude deep convection and deep-water formation associated with the AMOC drives the North Atlantic Current and accelerates the Gulf Stream, thereby contributing to the steep dynamic SSH gradient on the east coast of the United States. In addition to the dynamic sea level, the AMOC is also closely linked to the steric sea level[10] (see the Methods section for terminologies). Owing to the deep-water formation, the entire ocean column in the northern North Atlantic is occupied by very dense sea water, thereby significantly lowering the sea level. Model simulations suggest that a collapse of the AMOC could cause a large regional sea-level rise (SLR) in the North Atlantic[3].

Here we report a rapid SLR on the northeast coast of the United States during the twenty-first century projected by the climate models used for the Intergovernmental Panel on Climate Change (IPCC) Fourth Assessment Report (AR4). The projected ensemble mean (ten models) shows that the SLR during the twenty-first century is uneven, with some regions such as the northeast coast of the United States experiencing rises considerably faster and larger than the global mean (Fig. 1). In addition, the northeast coast

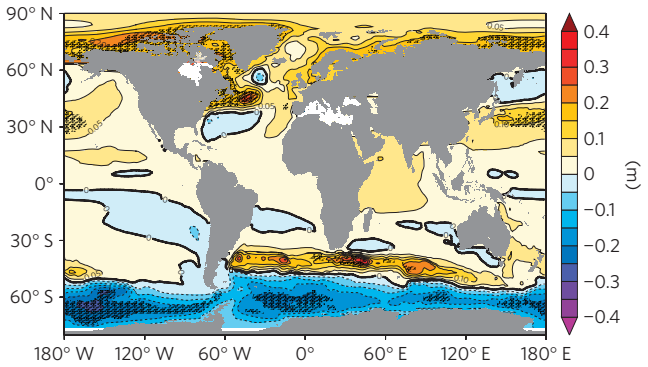

Figure 1 | Multi-model ensemble mean projection of the dynamic sea level. The values show the mean change (2091–2100 relative to 1981–2000) projected by ten AR4 climate models under the A1B scenario. Stippling indicates the regions where the ensemble mean divided by the ensemble standard deviation is greater than two. See Supplementary Fig. S1 for the models used in the calculation of the ensemble mean and their projections.

of the United States is a region where models agree in projecting the dynamic sea level. The sharp gradient of the dynamic sea-level change across the Gulf Stream and North Atlantic Current, and the rapid dynamic SLR on the northeast coast of the United States are robust features of the twenty-first century climate change (see Supplementary Fig. S1). Compared with the IPCC AR4 (ref. 1, Fig. 10.32), the robustness of this dynamic SLR is improved because some models unsuitable for the present study are excluded from the ensemble (see Supplementary Fig. S2).

Here we use the GFDL CM2.1 climate model to better understand the dynamic SLR on the northeast coast of the United States. We use the GFDL CM2.1 as a representative because the full data sets of CM2.1 are easily accessible and extra experiments are available. CM2.1 (see the Methods section for model information) has been used extensively for the IPCC AR4 integrations, including the climate projections under A2 (high), A1B (medium) and B1 (low) greenhouse-gas (GHG) emission scenarios[1]. With the increase of the GHG concentration in CM2.1, the global mean surface air temperature increases by 2.8 °C, 2.1 °C and 1.2 °C respectively in the A2, A1B and B1 scenarios during the twenty-first century (Fig. 2a). Owing to the changes in the thermohaline (heat and freshwater) fluxes in the high-latitude North Atlantic, the AMOC weakens from 22.6 Sv (1 Sv = 10^6 m^3 s^{-1}) in 1981–2000 to 13.0 Sv, 13.3 Sv and 15.2 Sv by the end of the twenty-first century in the three scenarios (Fig. 2a), representing relative weakenings of

[1]Center for Ocean-Atmospheric Prediction Studies, Florida State University, Tallahassee, Florida 32306, USA, [2]Climate Research Group, Department of Atmospheric Sciences, University of Illinois at Urbana-Champaign, Urbana, Illinois 61801, USA, [3]Geophysical Fluid Dynamics Laboratory, National Oceanic and Atmospheric Administration, Princeton, New Jersey 08542, USA. *e-mail: yin@coaps.fsu.edu.

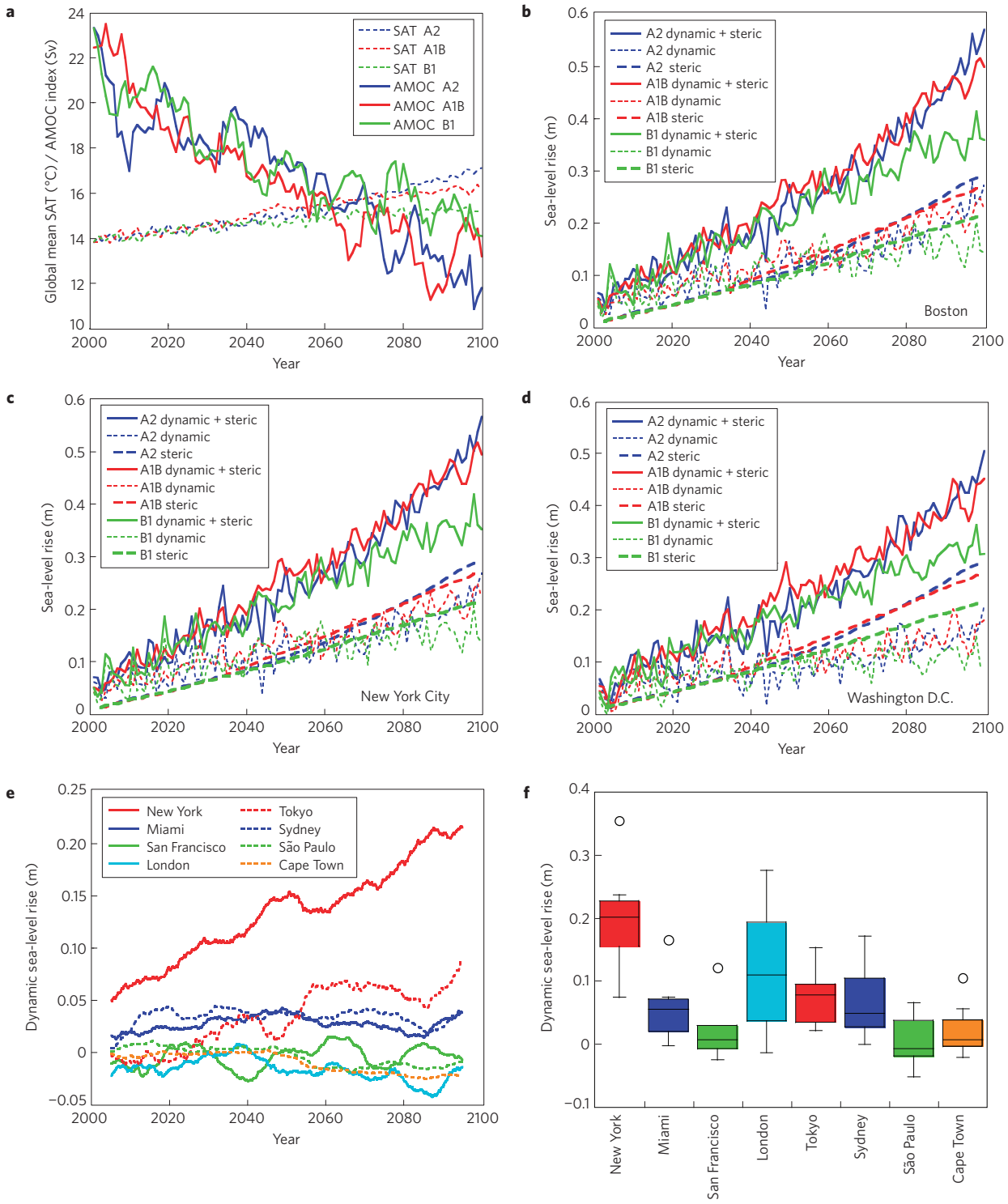

Figure 2 | Climate projections by the GFDL CM2.1. a, Global mean surface air temperature (SAT) and the AMOC. **b**–**d**, The SLRs at Boston (**b**), New York City (**c**) and Washington DC (**d**) relative to 1981–2000. **e**, The dynamic SLRs (ten year running mean) at coastal cities worldwide in the A1B scenario. **f**, The dynamic SLR projections (2091–2100) by ten AR4 models. The central line, top and bottom of each box, and top and bottom of each whisker, respectively, represent the median, 75th and 25th percentile, and 95th and 5th percentile values in the ensemble. The circles are extreme and unusual points. The AMOC index is the maximum overturning streamfunction value at 45° N in the Atlantic.

43%, 41% and 33%. These weakenings of the AMOC are in line with those estimated by IPCC AR4 (ref. 1) and the Coupled Model Intercomparison Project based on a model ensemble[2].

The simulated dynamic SSH during the 1990s is realistic compared to the observation[11], especially in terms of the sharp SSH gradient across the narrow Gulf Stream and North Atlantic Current (Fig. 3a,b). The very low sea level associated with the cyclonic subpolar gyre extends to the northeast coast of the United States. The weakening of the AMOC leads to a significant decline of the SSH gradient, and a rapid dynamic SLR on the northeast coast of North America during the twenty-first century (Fig. 3c–e and Supplementary Fig. S3). The dynamic SLR is relatively

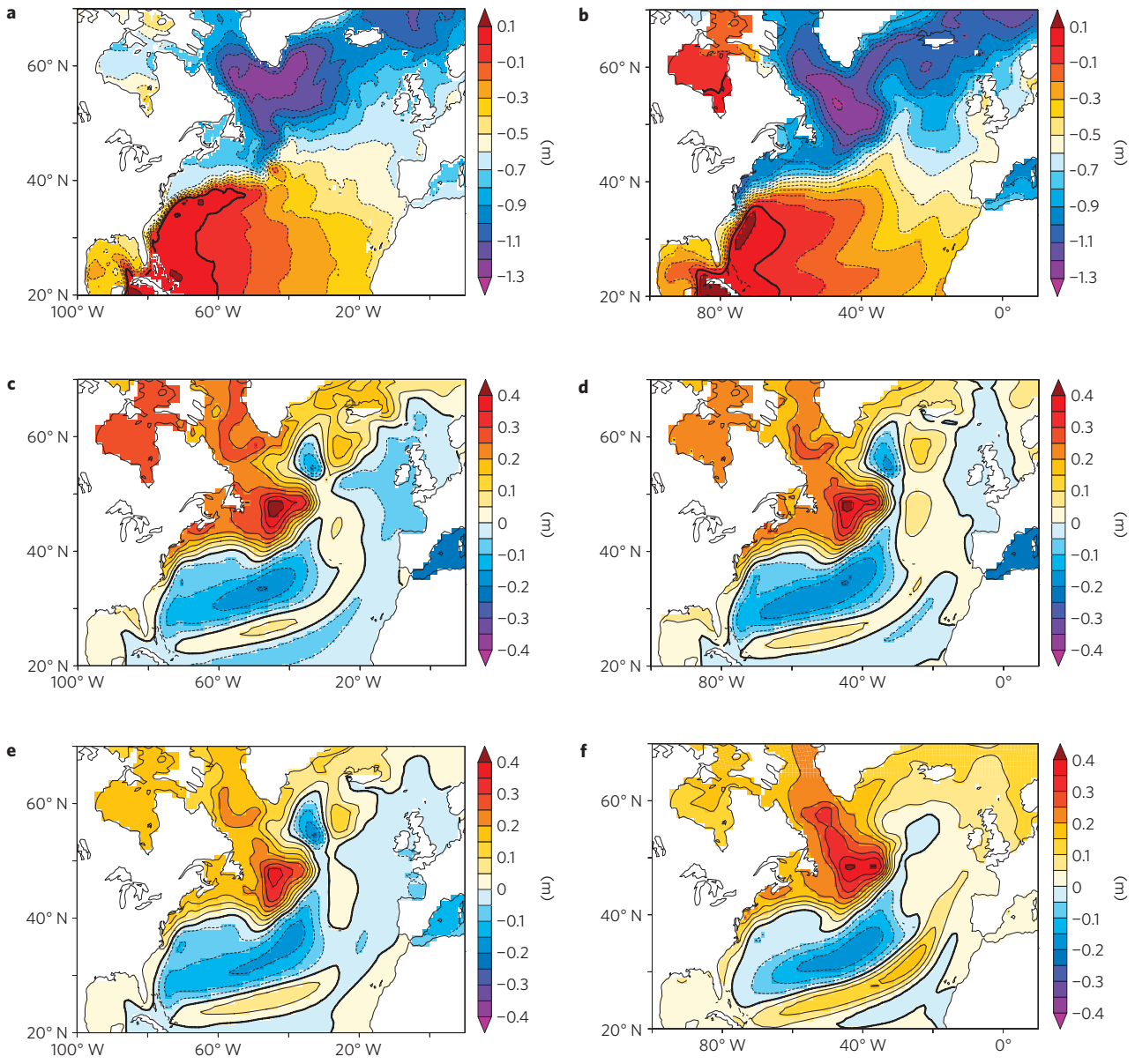

Figure 3 | Dynamic sea levels in the GFDL CM2.1. a, Observation[11] (1992–2002). **b**, Simulation (1992–2002). **c**–**e**, Projected anomalies (2091–2100 relative to 1981–2000) in the A2 (**c**), A1B (**d**) and B1 (**e**) scenarios. **f**, The dynamic sea-level change induced by an idealized 0.1 Sv freshwater input (water-hosing) into 50°–70° N of the Atlantic for 100 years (the mean of years 2091–2100 compared with the control). In the water-hosing run, radiative forcing is kept constant at the 1990 level and the global mean SLR induced by the global ocean mass increase is removed. The AMOC weakens by 37% over 100 years.

scenario independent. The maximum dynamic SLR occurs east of Newfoundland, with significant rises extending to the coastal region north of Cape Hatteras.

The dynamic SLR is mainly a result of the cessation of the deep convection and deep-water formation in the Labrador Sea, and the slowdown of the subpolar gyre. During 1981–2000, vigorous deep convection occurs in the Labrador Sea, which can reach more than 1,000 m depth (see Supplementary Fig. S4). Owing to ocean surface warming and freshening, the deep convection in the Labrador Sea shuts down by the end of the twenty-first century in all three scenarios. Compared with other sites, the deep convection in the Labrador Sea is very sensitive to the anomalies of the thermohaline fluxes[5], which probably results from positive feedbacks operating in this region[12]. The subpolar gyre weakens significantly with a northeastward shift of the barotropic (vertically independent) streamfunction pattern (see Supplementary Fig. S4). A fall of the dynamic sea level in the subtropical gyre and a North Atlantic dipole pattern[13,14] are also evident in Fig. 3c–e.

The dynamic SLR on the northeast coast of the United States is closely related to the horizontal gradient of the steric SLR and mass redistribution in the ocean (Fig. 4). In addition to global thermal expansion, the weakening of the formation and southward propagation of North Atlantic Deep Water causes a deep warming and extra steric SLR along the route of the deep western boundary current (Fig. 4a). From the maximum rise of about 0.35 m east of Newfoundland, the magnitude of this steric SLR reduces southward. In contrast, the steric SLR on the continental shelf is small owing to the shallow water column. The sharp steric SLR gradient across the shelf break (near the zero contour lines in Fig. 4) cannot be balanced by geostrophic currents, therefore leading to an increase in mass loading near the northeast coast of the United States (Fig. 4b). At Boston, New York City and

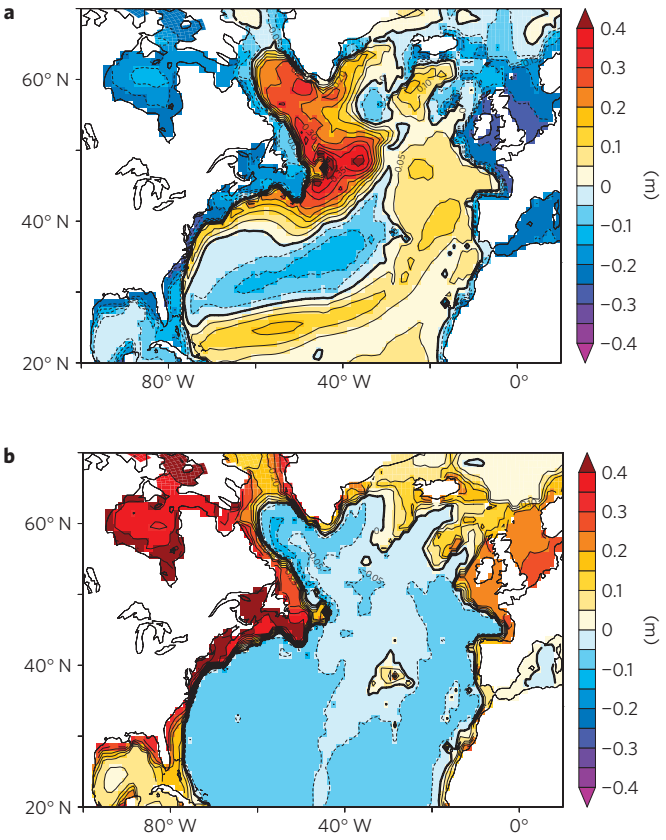

Figure 4 | Contributions of the steric effect and ocean mass redistribution to the dynamic SLR. a, The steric SLR. **b**, The SLR induced by mass redistribution. The SLRs show the mean of 2091–2100 relative to 1981–2000 in the A1B scenario run with the GFDL CM2.1. To better show the horizontal gradient of the steric SLR, the global mean steric SLR is subtracted in **a**. Mass redistribution is calculated on the basis of the change in the ocean bottom pressure.

Washington DC, mass redistribution and the local steric effect contribute oppositely to the dynamic SLR, whereas the impact of the atmospheric inverted barometer effect is very small[15] (see Supplementary Fig. S5).

A very similar pattern of the dynamic sea-level change also occurs in the 'water-hosing' experiment[5,16] (Fig. 3f). A slowdown of the AMOC induced by a 0.1 Sv freshwater addition in the deep-water-formation region causes a dynamic SLR on the northeast coast of the United States that resembles those in the IPCC scenario runs (Fig. 3c–f and Supplementary Fig. S6). The pattern correlation coefficient is 0.91 between Fig. 3d and f (20°–80° W, 30°–60° N). As a key process, the regional steric SLR along the deep western boundary current is also pronounced in the water-hosing experiment (see Supplementary Fig. S7). The comparison with the water-hosing run and the mechanism analysis indicates that the weakening of the AMOC has a dominant role in causing the dynamic SLR in the scenario runs, whereas the role of the wind change over the subtropical gyre is secondary (see Supplementary Fig. S8). The maximum potential of the dynamic SLR can be illustrated by the 1.0 Sv water-hosing experiment. 1.0 Sv freshwater addition is sufficiently large to shut down the AMOC, leading to a dynamic SLR of up to 1.5 m in the northern Atlantic, with a 1.2 m rise along the northeast coast of the United States (see Supplementary Fig. S6).

Although the dynamic SSH is an accurate description of the model's horizontal sea-level gradient, the global mean SLR and isostatic adjustment[17] must be taken into account to obtain the total regional SLR (see the Methods section). Owing to ocean warming, the global steric SLRs over the twenty-first century are 0.28, 0.26 and 0.21 m in the A2, A1B and B1 scenarios (Fig. 2), respectively, which are consistent with previous estimates[18,19]. As CM2.1 does not incorporate an ice sheet/glacier model, the SLR induced by the melting of small glaciers, ice caps and ice sheets can be estimated only indirectly[20]. On the basis of synthesis and observational sensitivity, the latest IPCC estimate of the land ice contribution to global SLR in the twenty-first century ranges from 0.03 to 0.33 m (ref. 1). The wide range is because the dynamics of ice sheets is largely unknown. A contribution above 2 m during this century can be excluded[21]. However, the upper bound of the estimate of the global mean SLR could reach 1.4 m in a study based on a semi-empirical approach[22].

Consequently, the dynamic SLR on the northeast coast of the United States is projected to have the same order of magnitude as the global steric and mass component. At New York City, for example, the dynamic SLRs projected by CM2.1 in the twenty-first century are 0.23 (0.21) m, 0.21 (0.20) m and 0.15 (0.15) m in the A2, A1B and B1 scenarios (the numbers in brackets give the multi-model ensemble mean). These SLRs greatly enhance the total increase, especially after 2050. By the end of the twenty-first century in CM2.1, the sum of the dynamic and steric SLRs in the three scenarios can reach 0.52, 0.48 and 0.37 m at Boston; 0.51, 0.47 and 0.36 m at New York City; and 0.44, 0.42 and 0.33 m at Washington DC (Fig. 2b–d). The total SLR at New York City could be further enhanced by local isostatic subsidence[17].

Other AR4 models show that the dynamic SLR on the northeast coast of the United States is qualitatively highly robust, although the magnitude varies (Fig. 2f and Supplementary Fig. S9). The spread in magnitude is a result of many differences between models. Compared with those at many other coastal cities, the dynamic SLR at New York City is large, with relatively small model-to-model variation (Fig. 2f). This indicates that the uncertainty is relatively small on the northeast coast of the United States (Fig. 1), with the result from the GFDL CM2.1 close to the ensemble mean. Linear regression lines fit the AR4 model results well within the range of available data (see Supplementary Fig. S9).

Although a large dynamic SLR (~1 m) in the entire North Atlantic can be induced by a collapse of the AMOC (ref. 3), climate models project only a moderate dynamic rise (~0.2 m) during this century. More importantly, our results indicate that the dynamic sea level on the northeast coast of the United States is particularly sensitive to the increase in the GHG concentration, whereas the dynamic sea-level change along the European coast cannot be assessed with confidence owing to model uncertainty (Figs 1 and 2f).

Our results show that the northeast coast of the United States is among the most vulnerable regions to future changes in sea level and ocean circulation, especially when considering its population density and the potential socioeconomic consequences of such changes. It should be noted that the impact of the melting of the Greenland ice sheet on the AMOC is not taken into account here. We believe that including extra meltwater from the Greenland ice sheet would increase the SLR directly and further weaken the AMOC, strengthening the main conclusion found here. The rapid SLR would put cities such as New York at greater risk of coastal hazards such as hurricanes and intense winter storm surges[7–9]. Given that the next IPCC assessment (AR5) will focus on regional climate and extreme events, including regional sea level[23], our results support a focused effort to understand regional climate change mechanisms and magnitudes.

Methods

GFDL CM2.1 is a climate model that incorporates the atmosphere, land, ocean and sea-ice systems[24]. It realistically simulates many features of the climate system and has been assessed systematically[25,26]. In particular, the oceanic component is a relatively high-resolution, free-surface general circulation model, which explicitly

represents the freshwater flux at the ocean surface. It uses 1° horizontal resolution with the meridional resolution gradually enhanced to 1/3° in the tropics. It has 50 levels with 22 levels in the upper 220 m. The dynamic sea level (η) in CM2.1 is a prognostic variable. The prognostic equation of η is

$$\eta_t = -\nabla \cdot \mathbf{U} + q_w$$
$$\mathbf{U} = \int_{-H}^{\eta} \mathbf{u}\, dz$$

where H is the ocean depth, q_w is the surface freshwater flux and $\mathbf{u}$ is the horizontal velocity. Owing to the Boussinesq approximation, η does not include the global SLR induced by the steric effect. The global steric SLR (h_s) can be accurately diagnosed on the basis of the three-dimensional time-varying density field:

$$h_s = -\frac{1}{S}\int_S \int_{-H}^{\eta} \frac{\Delta\rho}{\rho}\, dz\, dS$$

where ρ is the *in situ* seawater density and S is the surface area of the ocean. Previous research[27] has shown that h_s should be added to η to obtain the total regional SLR.

The transient climate response (the change of the global mean surface temperature at the time of CO_2 doubling with a 1% yr^{-1} increase rate) of CM2.1 is 1.6 °C (ref. 28), which is close to the median of the coupled models used for the IPCC AR4 (ref. 29). The AMOC in CM2.1 also shows a medium sensitivity to external thermohaline forcings[5].

In this study, the term 'dynamic' refers to the geostrophic balance between the SSH gradient and horizontal currents, whereas 'steric' refers to the specific volume of sea water, which is a function of temperature, salinity and pressure. The dynamic sea level shows the deviation from the global mean. It should be noted that the dynamic and steric SLRs are closely related:

$$\eta = h_s' + h_a + h_b$$

where h_s' is the local steric SLR deviation, h_a is the barometric correction and h_b is the contribution from the bottom pressure change. The inverted barometer effect (h_a) is not included in the calculation of the dynamic sea level in CM2.1. Its contribution can be estimated on the basis of the change in sea-level pressure.

Received 13 October 2008; accepted 10 February 2009; published online 15 March 2009

References

1. Meehl, G. A. *et al.* in *Climate Change 2007: The Physical Science Basis. Contribution of Working Group I to the Fourth Assessment Report of the Intergovernmental Panel on Climate Change* (eds Solomon, S. *et al.*) 747–845 (Cambridge Univ. Press, 2007).
2. Gregory, J. M. *et al.* A model intercomparison of changes in the Atlantic thermohaline circulation in response to increasing atmospheric CO_2 concentration. *Geophys. Res. Lett.* **32**, L12703 (2005).
3. Levermann, A., Griesel, A., Hofmann, M., Montoya, M. & Rahmstorf, S. Dynamic sea level changes following changes in the thermohaline circulation. *Clim. Dyn.* **24**, 347–354 (2005).
4. Douglas, B. C., Kearney, M. S. & Leatherman, S. R. (eds) *Sea Level Rise: History and Consequences* (Academic, 2001).
5. Stouffer, R. J. *et al.* Investigating the causes of the response of the thermohaline circulation to past and future climate changes. *J. Clim.* **19**, 1365–1387 (2006).
6. Vellinga, M. & Wood, R. A. Impacts of thermohaline circulation shutdown in the twenty-first century. *Clim. Change* **54**, 251–267 (2002).
7. Colle, B. A. *et al.* New York City's vulnerability to coastal flooding. *Bull. Am. Meteor. Soc.* **89**, 829–841 (2008).
8. Gornitz, V., Couch, S. & Hartig, E. K. Impacts of sea level rise in the New York City metropolitan area. *Glob. Planet. Change* **32**, 61–88 (2001).
9. Jacob, K., Gornitz, V. & Rosenzweig, C. in *Managing Coastal Vulnerability* (eds McFadden, L., Nicholls, R. & Penning-Rowsell, E.) 139–156 (Elsevier, 2007).
10. Knutti, R. & Stocker, T. F. Influence of the thermohaline circulation on projected sea level rise. *J. Clim.* **13**, 1997–2001 (2000).
11. Maximenko, N. A. & Niiler, P. P. in *Recent Advances in Marine Science and Technology 2004* (ed. Saxena, N.) 55–59 (PACON International, 2005).
12. Levermann, A. & Born, A. Bistability of the Atlantic subpolar gyre in a coarse resolution climate model. *Geophys. Res. Lett.* **34**, L24605 (2007).
13. Bryan, K. The steric component of sea level rise associated with enhanced greenhouse warming: A model study. *Clim. Dyn.* **12**, 545–555 (1996).
14. Landerer, F. W., Jungclaus, J. H. & Marotzke, J. Regional dynamic and steric sea level change in response to the IPCC-A1B scenario. *J. Phys. Oceanogr.* **37**, 296–312 (2007).
15. Stammer, D. & Huttemann, S. Response of regional sea level to atmospheric pressure loading in a climate change scenario. *J. Clim.* **21**, 2093–2101 (2008).
16. Yin, J. & Stouffer, R. J. Comparison of the stability of the Atlantic thermohaline circulation in two coupled atmosphere-ocean general circulation models. *J. Clim.* **20**, 4293–4315 (2007).
17. Peltier, W. R. in *Sea Level Rise: History and Consequences* (eds Douglas, B. C., Kearney, M. S. & Leatherman, S. P.) 65–95 (Academic, 2001).
18. Gregory, J. M. *et al.* Comparison of results from several AOGCMs for global and regional sea-level change 1900–2100. *Clim. Dyn.* **18**, 225–240 (2001).
19. Meehl, G. A. *et al.* How much more global warming and sea level rise? *Science* **307**, 1769–1772 (2005).
20. Raper, S. C. B. & Braithwaite, R. J. Low sea level rise projections from mountain glaciers and icecaps under global warming. *Nature* **439**, 311–313 (2006).
21. Pfeffer, W. T., Harper, J. T. & O'Neel, S. Kinematic constraints on glacier contributions to 21st-century sea-level rise. *Science* **321**, 1340–1343 (2008).
22. Rahmstorf, S. A semi-empirical approach to projecting future sea-level rise. *Science* **315**, 368–370 (2007).
23. Kintisch, E. IPCC tunes up for its next report aiming for better, timely results. *Science* **320**, 300 (2008).
24. Delworth, T. L. *et al.* GFDL's CM2 global coupled climate models. Part I: Formulation and simulation characteristics. *J. Clim.* **19**, 643–674 (2006).
25. Reichler, T. & Kim, J. How well do coupled models simulate today's climate? *Bull. Am. Meteor. Soc.* **89**, 303–311 (2008).
26. Gleckler, P. J., Taylor, K. E. & Doutriaux, C. Performance metrics for climate models. *J. Geophys. Res.* **113**, D06104 (2008).
27. Greatbatch, R. J. A note on the representation of steric sea level in models that conserve volume rather than mass. *J. Geophys. Res.* **99**, 12767–12771 (1994).
28. Stouffer, R. J. *et al.* GFDL's CM2 global coupled climate models. Part IV: Idealized climate response. *J. Clim.* **19**, 723–740 (2006).
29. Randall, D. A. *et al.* in *Climate Change 2007: The Physical Science Basis. Contribution of Working Group I to the Fourth Assessment Report of the Intergovernmental Panel on Climate Change* (eds Solomon, S. *et al.*) 589–662 (Cambridge Univ. Press, 2007).

Acknowledgements

We thank T. L. Delworth, J. M. Gregory, A. Hu, T. F. Stocker, G. A. Vecchi and M. Winton for comments and suggestions. We also thank many others at GFDL for carrying out the IPCC AR4 integrations and providing computer and model support. We acknowledge other climate modelling groups, the Program for Climate Model Diagnosis and Intercomparison (PCMDI), the WCRP's Working Group on Coupled Modelling (WGCM) and the Office of Science, US Department of Energy. J.Y. is supported by the US Department of Energy (Grant No. DE-FG02-07ER64470).

Additional information

Supplementary Information accompanies this paper on www.nature.com/naturegeoscience. Reprints and permissions information is available online at http://npg.nature.com/reprintsandpermissions. Correspondence and requests for materials should be addressed to J.Y.